Electronic Supplementary Material (ESI) for Physical Chemistry Chemical Physics.

Supporting Information for

Multiphoton emission of single CdZnSe/ZnS quantum dots coupled with plasmonic Au nanoparticles

Luogang Xie*, Hongjun Yang, Yang Yang, Ziyang Chen, Hangtian Li, Zijiong Li and Dewei Liu

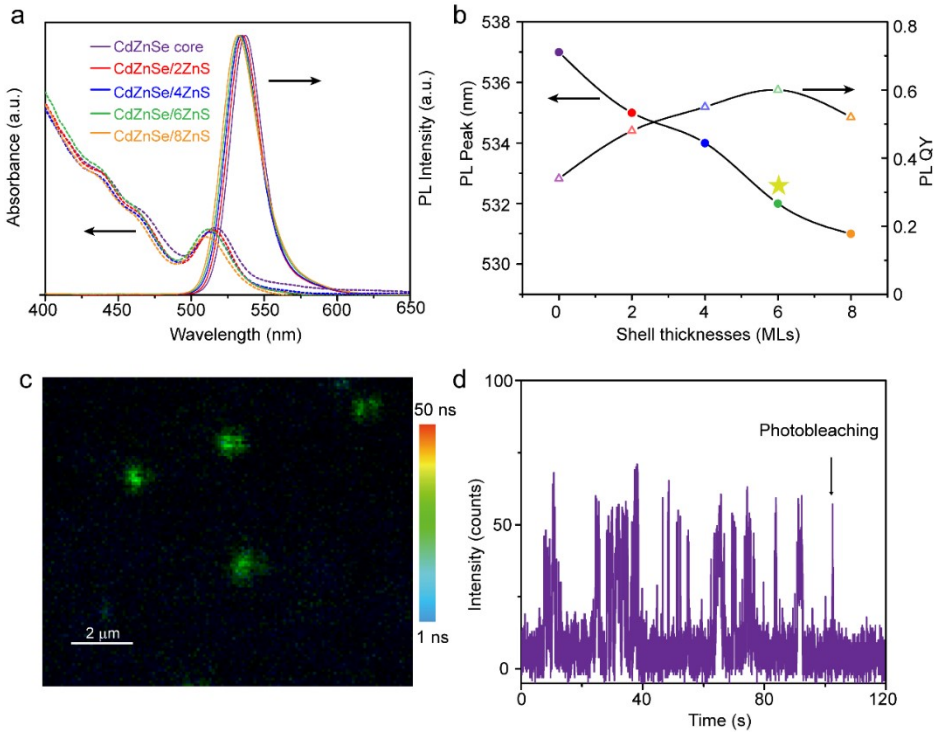

Fig. S1 (a) Absorbance (dashed lines) and PL spectra (solid lines) of CdZnSe core and CdZnSe/ZnS QDs with different ZnS shell thicknesses from 2 ML to 8 MLs. (b) The shell thickness dependence of PL peak (solid circle) and PL QY (open triangle) for the core and core/shell QDs. (c) FLIM image of single CdZnSe core QDs embedded in PMMA matrix. (d) Representative fluorescence blinking of single CdZnSe core QD at the excitation power of 20 nW.

To obtain the suitable QDs that match the localized surface plasmon (LSP) resonance band of Au nanoparticles, we have designed and synthesized a series of green-emitting CdZnSe/ZnS QDs with different shell thicknesses. The alloyed CdZnSe core is capped with a wide bandgap ZnS shell to form the core-shell structure, which can passivate the surface defect of the core and improve the PLQYs and photostability. Fig. S1a displays the steady-state UV-vis absorption and PL spectra of CdZnSe/ZnS QDs with a shell thickness of 0 ~ 8 monolayer (ML) in toluene. The absorption and PL peak were slightly blue-shifted with increasing ZnS shell, verifying the good confinement of excitons by

the wide bandgap of the ZnS shell. The absolute PL QYs of QDs samples in toluene were further measured using a quantum efficiency measurement system with an integrating hemisphere. Fig. S1b presents the evolution of the PL peak and PL QYs of CdZnSe/ZnS QDs with increasing shell thickness. The PL peak was blue-shifted from 537 nm in bare CdZnSe cores to 531 nm in CdZnSe/8ZnS QDs. The PL QYs of CdZnSe/ZnS QDs increase as the shell layer thickness increases from 0 to 6 MLs, but decreases when it is 8 MLs. A maximum QY of 60% is observed when the ZnS shell layer is 6 MLs. This increase in QYs can be attributed to the passivation of CdZnSe core surface defects by capped ZnS shell, and the decrease for the thicker ZnS shell (8 MLs) originates from the increased defects at the interfaces of core/shell induced by the increased lattice strain. Furthermore, the CdZnSe/6ZnS QDs own preferably photostability which facilitates the study at the single particle level. As a control, the single CdZnSe core QDs have been studied at the single particle level. The fluorescence lifetime imaging microscopy (FLIM) image of monodispersed CdZnSe core QDs and typical PL blinking trace are shown in Fig. S1c and S1d. The single core QD exhibits dramatically blinking behavior and photobleaching properties even if they are protected by PMMA, indicating that core QDs without passivation by the shell are relatively difficult for single particle study and further statistical analysis. Taking these factors into consideration, we choose the CdZnSe/6ZnS QDs with the PL peak of 532 nm and 60% PLQY as a model system to investigate the modulation of LSP on the photon emission behaviors.

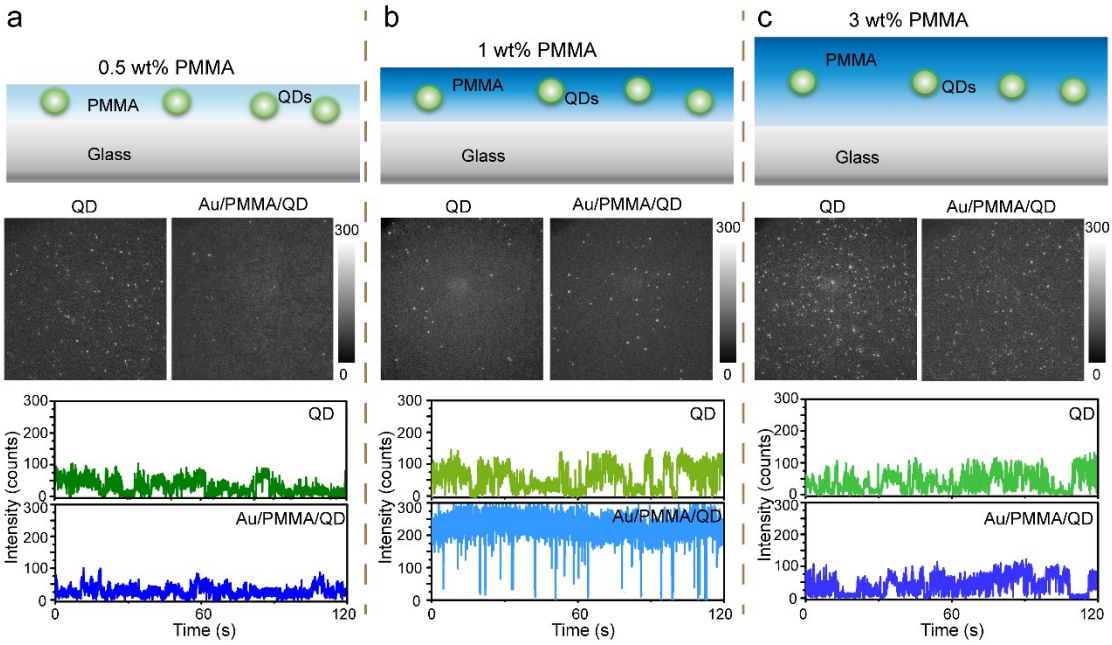

Fig. S2 The dependence of photon emission behavior of single QDs on the PMMA solution weight concentration (a) 0.5 wt% (b) 1 wt% and (c) 3 wt%. Schematic diagram of sample configurations (top), fluorescence intensity images of single QDs before and after Au nanoparticles deposition (middle), and blinking traces of single QDs before and after Au nanoparticles deposition (bottom), respectively.

To achieve PL fluorescence enhancement with the optimal distance between QDs and Au nanoparticles, the thickness of the PMMA film was controlled by adjusting the PMMA solution. The dilute QDs with the same concentration were added into the PMMA solution with weight concentrations of 0.5 wt%, 1 wt%, and 3 wt%, respectively, followed by spin-coating on a cover glass. The schematic diagrams of sample configuration under different scenarios and the corresponding fluorescence intensity images of single QDs without/with Au nanoparticles are shown in Fig. S2, and the PMMA thickness is regarded as the average distance between plasmon nanostructures and QDs.[1-3] When the thickness of PMMA is thin (Fig. S2a), the fluorescence intensity quenching was observed with a reduced number of fluorescent spots for Au/PMMA/QDs (middle in Fig. S2a), and the fluorescence intensity of the remaining quantum dots is weaker than that for the QDs without Au nanoparticles (bottom in Fig. S2a). When the thickness of PMMA is increased, the fluorescent intensity of single QDs after Au nanoparticles deposition exhibits significant

enhancement, and the blinking is obviously suppressed (bottom in Fig. S2b). Meanwhile, when the thickness of PMMA is too thick, the modulation of the LSP on the photon emission behavior of single QDs is negligible. As shown in Fig. S2c, the fluorescent intensity and blinking are almost unaffected by the LSP of Au nanoparticles. Hence, the PMMA solution of 1 wt% is the optimized condition to enhance the PL intensity of single QDs coupled with the LSP of Au nanoparticles.

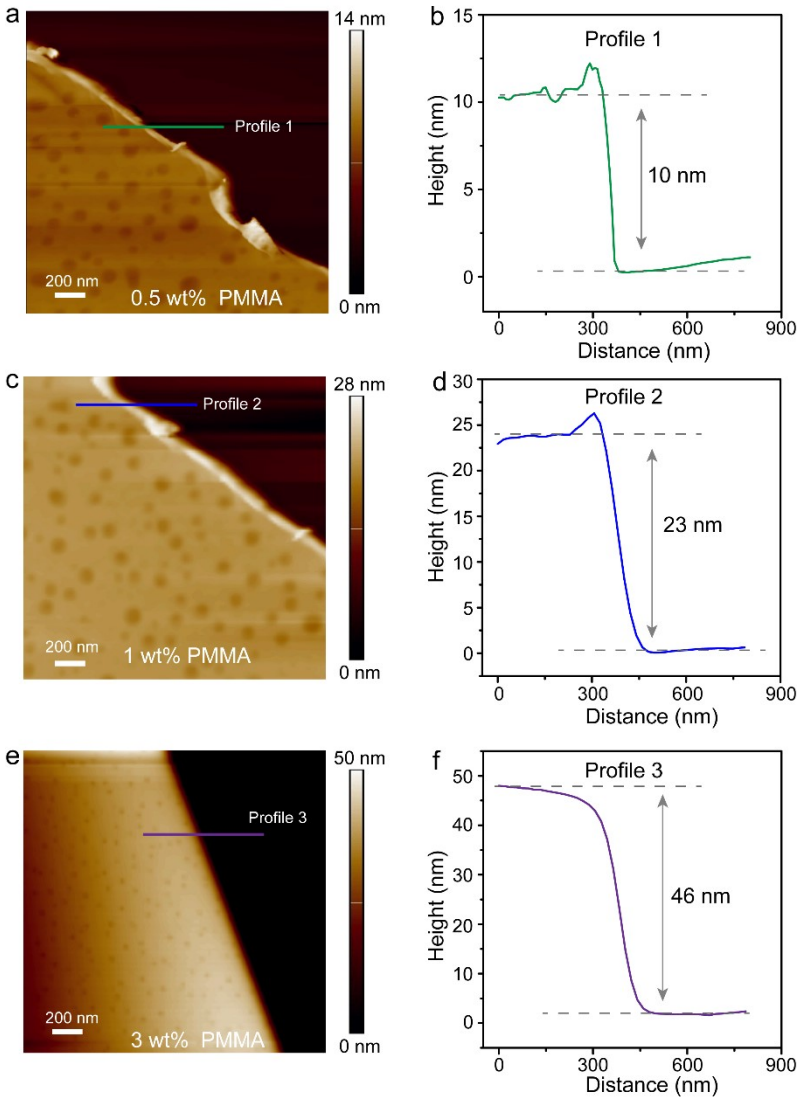

Fig. S3 AFM images and corresponding height profiles for the PMMA films in the cut-off area prepared with weight concentrations of 0.5 wt% (a, b), 1 wt% (c, d), and 3 wt% (e, f), respectively.

The thicknesses of the PMMA layers, which are prepared by spin-coating PMMA solution onto mica with different weight concentrations (0.5 wt%, 1 wt%, and 3 wt%), are further estimated using the atomic force microscopy (AFM). Fig. S3 shows the AFM images and profiles of PMMA films in the cut-off areas of the three samples. The

surface structures of all PMMA films are found to be relatively smooth. The thickness of the 0.5 wt% PMMA thin film is approximately 10 nm, while that of the 1 wt% PMMA film is 23 nm, and the 3 wt% PMMA film is 46 nm.

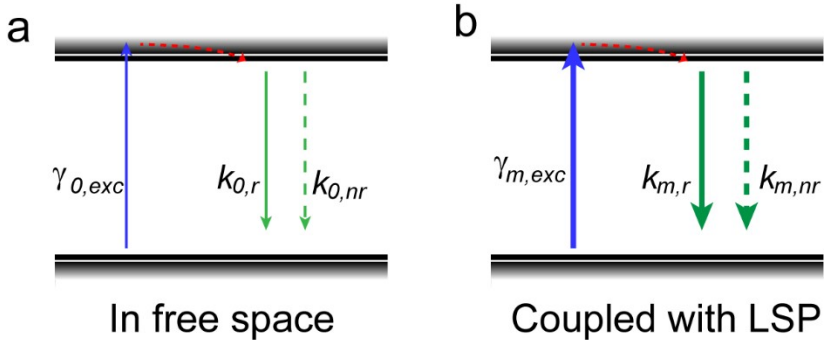

Fig. S4 Energy structure schematic shows the excitation and emission processes of single QD in free space (a) and coupled with LSP of Au nanoparticles (b). The bold arrows in (b) represent the enhanced excitation and emission.

The absorption and emission spectrums of the QDs overlap the LSP band of the Au nanoparticles, which is beneficial for the enhancement of the excitation rate and radiative decay rate. When the LSP resonance band of the metal nanoparticle overlaps the absorption spectrum of the nearby emitter, the excitation rate of the emitter is enhanced by the electric field of the LSP. When the LSP resonance band overlaps with the emission spectrum of the emitter, the radiative and nonradiative processes of the emitter are enhanced. The enhancement factor of excitation rate $\eta_{exc} = \gamma_{exc}/\gamma_{0,exc}$ and radiative rate $\eta_r = k_r/k_{r,0}$ can be deduced by the theory of plasmon-enhanced fluorescence, and the excitation and emission processes of single QD in free space and coupled with LSP are shown in Fig. S4.

After the absorption of a photon, an electron in a single QD is excited to a higher energy state, and then the excited QD relaxes the energy via radiative decay (photon emission) or via a nonradiative recombination channel (Fig. S4a). The PL intensity of a single QD can be expressed as $I_0 = \gamma_{0,exc}\phi_0$, where $\gamma_{0,exc}$ is the excitation rate and ϕ_0 is the quantum yield. The ϕ_0 is calculated by $\phi_0 = \frac{k_{0,r}}{k_{0,r} + k_{0,nr}}$, where $k_{0,r}$ and $k_{0,nr}$ are the radiative and nonradiative decay rates, respectively. The lifetime of the excited

electron state is given by $\tau_0 = \frac{1}{k_{0,r} + k_{0,nr}}$.

When the single QD is coupled with an Au nanoparticle, the PL intensity will be modified in the excitation process and emission process. For simplification, the QD and the Au nanoparticle are treated as a hybrid system. The enhanced excitation rate and enhanced radiative and nonradiative decay rates are drawn in Fig. S4b. Similarly, for single coupled QD, PL intensity, quantum yield, and lifetime can be expressed as $I_m = \gamma_{m,exc}\phi_m$, $\phi_m = \frac{k_{m,r}}{k_{m,r} + k_{m,nr}}$, and $\tau_m = \frac{1}{k_{m,r} + k_{m,nr}}$, respectively. The subscript *m* represents the QD coupled with LSP. Hence, the enhancement factor of excitation rate η_{exc} and radiative rate η_r can be expressed as follows,

$$\eta_{exc} = \frac{\gamma_{m,exc}}{\gamma_{0,exc}} = \frac{I_m \cdot \phi_0}{I_0 \cdot \phi_m} \quad (1)$$

$$\eta_r = \frac{k_{m,exc}}{k_{0,exc}} = \frac{\phi_m \cdot \tau_0}{\phi_0 \cdot \tau_m} \quad (2)$$

If the I, ϕ and τ for QD in free space and coupled with LSP were measured, we can obtain the value of η_{exc} and η_r, respectively. The parameters of I and τ can be conveniently obtained in single particle experiments and the ϕ can be measured using the standard method of integrating spheres. The ϕ_0 of CdZnSe/ZnS QDs in toluene is 60% measured with a QE-2100 (Otsuka Photal Electronics) equipped with an integrating hemisphere. Unfortunately, the ϕ_m of Au/PMMA/QDs sample cannot be detected, for that the concentration of the QDs (~10^{-8} M) for single-dot dispersion is too low to generate enough photons for the absolute PL QYs measurement. However, the increased ϕ_m of QDs coupled with LSP can be indirectly deduced by the suppressed photoluminescence blinking. Hence, η_{exc} and η_r can be calculated using I_0 = 80 counts, I_m = 250 counts, τ_0 = 15 ns, τ_m = 2 ns and ϕ_0 = 0.6 as the average values of the data shown in Fig. 6 in the revised manuscript. If ϕ_m is in the range of 0.6-1, the η_{exc} is estimated to be 2-3, and η_r is estimated to be 7-12. The estimated η_r is larger than the actual value, because the energy transfer channel (Forster energy transfer) of exciting

the localized plasmon resonance of the Au nanoparticle by excited QDs is ignored in the simplified model for the coupled QD in Fig. S4b. As a result, within an order of magnitude, the approximating excitation enhancement to radiative rate enhancement is used in this study, hence the enhancement factor for the radiative rate is written as $\eta_r \approx \sqrt{\frac{I}{I_0} \cdot \frac{\tau_0}{\tau}}$, and the calculated η_r in Fig. 7 is in the range of 2-5, which is close to the estimated value of η_{exc}.

References

1 H. Naiki, S. Masuo, S. Machida and A. Itaya, *J. Phys. Chem. C*, 2011, **115**, 23299-23304.

2 V. Krivenkov, S. Goncharov, P. Samokhvalov, A. Sánchez-Iglesias, M. Grzelczak, I. Nabiev and Y. Rakovich, *J. Phys. Chem. Lett.*, 2019, **10**, 481-486.

3 S. J. LeBlanc, M. R. McClanahan, M. Jones and P. J. Moyer, *Nano Lett.*, 2013, **13**, 1662-1669.